Hindawi
Journal of Nanomaterials
Volume 2023, Article ID 1008046, 10 pages
https://doi.org/10.1155/2023/1008046

Research Article

Influence of Process Parameters and Convective Heat Transfer on Thermophysical Properties of SiO_2 Nanofluids by Multiobjective Function Analysis (DFA)

R. Suprabha,[1] **C. R. Mahesha**,[1] **and C. E. Nanjundappa**[2]

[1]*Department of Industrial Engineering and Management, Dr. Ambedkar Institute of Technology, Bangalore 560056, India*
[2]*Department of Mathematics, Dr. Ambedkar Institute of Technology, Bangalore 560056, India*

Correspondence should be addressed to R. Suprabha; suprabha.im@drait.edu.in

Received 1 August 2022; Revised 5 October 2022; Accepted 24 November 2022; Published 27 January 2023

Academic Editor: R. Lakshmipathy

From the requirements, high-performance cooling systems in the applications of solar, heat exchangers, and chemical industries are needed to improve efficiency. The metal-oxides-based nanofluids composed the better thermal properties with exchange of heat-transfer mechanisms. Therefore, this study mainly focused on nanosilicon dioxide materials to produce the nanofluids with blending of water-base medium by two-step techniques. The scanning electron microscope was used to analyze the presence of silicon dioxide nanoparticles from the procured material. During the two-step method input aspects like weight fraction of silicon dioxide (1.5–4.5 wt%), particle sizes (10–30 μm), pH range of water (5–9), and sonication process time (2–4 hr) were considered. The outcomes like thermal conductivity, specific heat capacity, and viscosity were selected as thermal physical properties. The desirability techniques were implemented to identify the best optimal input parameters from the nanofluid processing. From the desirability outcomes, the processed nanosilicon dioxide fluids with respective input parameters were 0.9623 W/mK for thermal conductivity, 688 J/kg K forspecific heat capacity, and 0.00162 for viscosity, respectively. The heat-transfer coefficient was successfully identified with processed nanosilicon dioxide fluids, and the Nusselt number and Reynolds number were attained with respective heat-transfer coefficients.

1. Introduction

In the last decades, energy crisis is more consumed with requirements of energy applications such as electronic products, chemical industry, power plant engineering, food and beverage industries [1]. The subsequent achievements are highly influenced by the requirements like greater efficiency, multimode function, less weight, and compact shape [2]. The enhanced superior heat-transfer medium, or liquid, and the thermic liquid have significant scopes in the thermal-related engineering fields [3]. Thermal fluids have played an essential role in the process and system-based maintaining industries and employed with ideal running temperature [4]. Therefore, to improve the mechanical thermal efficiency, nanofluids are rich medium for heat-transfer liquid [5]. Due to this, it has secured colloidal scattering as compared with the solid-based nanoparticles; these particle sizes must be in the range of 1–100 nm during liquid process [6].

Some unique requirement is needed to select appropriate nanofluids. Those characteristics are compatibility, availability, thermal attributes, stability in chemical process, and less in price [7]. The conventional heat-transfer technique is insufficient to exchange the heat resulting in less thermophysical properties. To overcome this issue in the thermal- and heat-transfer managing led to identification of the effective nanofluid, and it is the most admired objective in this research [8]. Therefore, nanofluid is utilized to increase heat transfer and enhanced thermophysical properties. Hence, the thermalophysical properties fully depends up on the efficiency of cooling systems. So the researchers were highly involved in finding the better thermal conductivity in the presence of nanofluids [9]. The medium of nanoparticle with metal oxides have different concentrations

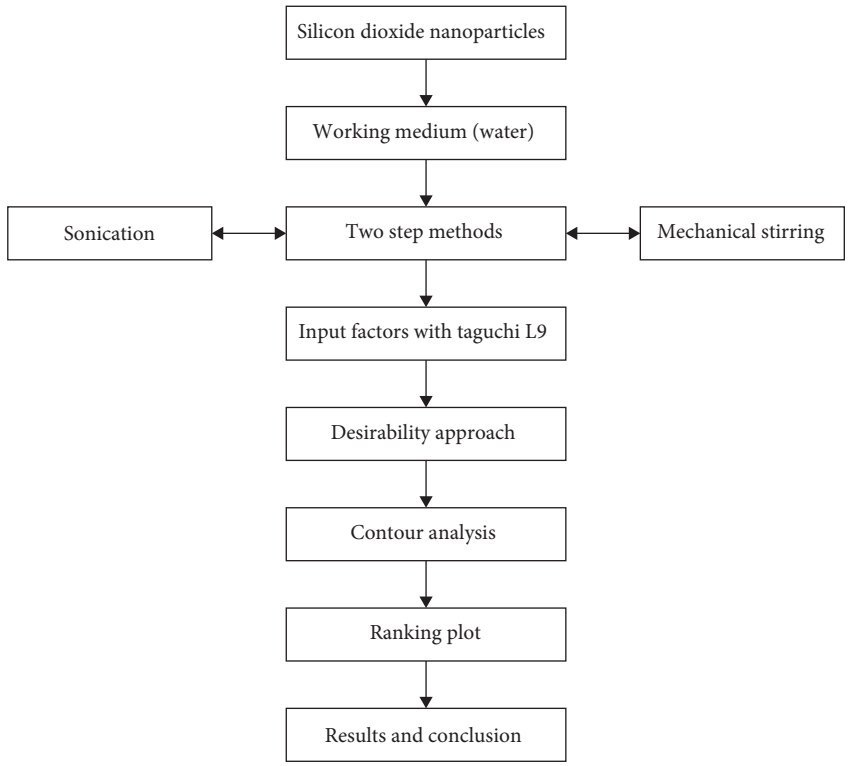

Figure 1: Experimental layout.

to achieve the nanofluids by the conventional technique. The different nanomaterials are graphite, carbon nanotubes, metal oxides, graphene oxides, metals, diamonds, carbides, graphenes, and nitrides [10]. Normally in the metal-based nano-fluids for nanoformulations, the thermal conductivity is lesser when compared with the base metals, and settling issues were developed during the nanofluid formulations [11]. In comparison with metals, metal-oxide-based nanomaterials showed better thermophysical properties. Formulation of nanofluid is very effective to produce maximum thermal conductivity and never compensates the pressure drop [12]. Therefore, the increasing of thermophysical properties enhances the heat-transfer mechanism. The hybrid nanofluid is composed between two or more than two metal oxide nanoparticles when suspended with traditional base liquids. Single- or mononano fluids were prepared from one nanoparticle of metal oxide dispersed in the base fluids [13]. Many techniques like glycols with water, glycols without water, and oils and water were used to compose the nanofluid formulation [14]. Among these methods, water was the majorly used to act as a coolant, and various investigations are focused more on water-based nanofluids by various authors [15]. The overview of experimental plan is displayed in Figure 1.

Abu-Hamdeh et al. [16] investigated the nanofluid of SiO_2 in various preparations in the heat exchangers. The main objective was to improve the efficiency in the solar power plant systems. It is concluded that the efficiency was increased at 25% when using SiO_2. Singh et al. [17] analyzed the various nanofluids like aluminum oxide, silicon dioxide and magnesium oxide to identify the thermal behaviors. The latent heat thermal energy storage system was used to complete the investigations properly. Among the metal oxides, SiO_2 provided better efficiency in this study. Jang et al. [18] studied the nanocoated SiO_2 on the steel in the concrete technology to improve the tensile and interfacial bonding. A comparision between the plain steel and coated nano-SiO_2 steel to improved the corrosion rate. Finally, the coated SiO_2 steel increased the bonding strength at 50%. Yu et al. [19] increased thermophysical properties in the thermal storage applications by the influence of SiO_2 nanofluids. The specific heat was enhanced at 2.58 times than the eutectic nitrate. Iqbal et al. [20] addressed the performance of engine-oil flow by using the nanosilicon carbide and silicon dioxide powders. These two nanopowders were suspended in the base fluid of engine oil and, in addition to that, the heat mechanism was migrated through the temperature conditions. Esfe et al. [21] studied the improvement of viscosity in the engine oil with help of multiwall carbon nanotubes and silicon dioxide nanoparticles. The engine performance was improved by 42.53% in the statistical analysis. The response surface methodology was used to forecast the experimental values. Awais et al. [22] enhanced the thermal conductivity in the kerosene oil with help of silicon dioxide and titanium dioxide. The Riga wedge technique was used to create the fluid formulations. SiO_2 nanofluid provides better thermal conductivity. In this research, two-step technique was implemented to produce the nanofluids with utilization of sonication and mechanical stirring process. The even dispersion of nanoparticles is very significant to enhance the interfacial bonding with maximum stability in the base fluids and was accomplished in the two-step technique [23]. These stability controls

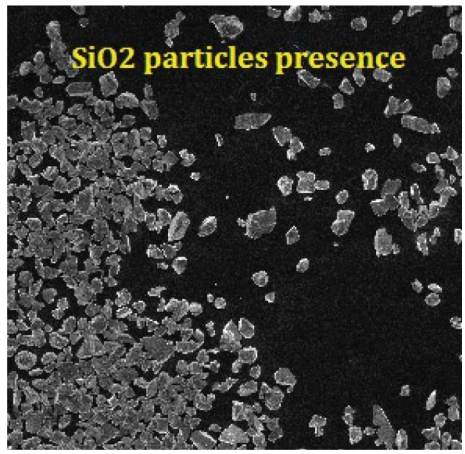

FIGURE 2: SiO_2 SEM micrograph.

were fully influenced by the frequency, temperature, and time of sonication method. The rising of nanoparticles and its concentration volumes improves the thermal conductivity in the prepared nanofluids. Based on the detail literature reviews, SiO_2 was considered for nanoparticle material and to produce the nanofluids along with water-base fluid by two-step technique. This research work aims to investigate the optimum process parameter of nano silicon dioxide materials to produce the nanofluids with the blending of water-base medium by two-step techniques.

2. Material and Preparation of Nanofluids Aspects

In this study, silicon dioxide has been chosen as a base metal oxide element with water (H_2O). It is suspended in base fluids. The particle size analyzer was used to check the size of the nanoparticle and selected sizes were 10–30 nm. The silicon dioxide was purchased at Coimbatore Metal Mart. The thermophysical properties of SiO_2 and water were as follows: 2,220 and 3,885 kg/m^3 densities, 703 and 731 J/kg K specific heat capacities, 1.2 and 40 W/mK thermal conductivities, respectively. The SEM analysis was employed to identify the presence of particle elements which is displayed in Figure 2. From Figure 2, it is clear that the silicon dioxide particles were observed.

The appropriate weight machine was used to measure the weight of SiO_2 particles from the manufacturers of Nitiraj. The two-step technique was used to conduct the nanofluid preparation accompanying the mechanical stirring and ultrasonication process to vanish the agglomerated particles in the working base fluid. To evaluate the essential volume concentration, 0.5 ml measuring flask was used. The parameters like amplitude (123 μm), 130 W and 40 kHz power was maintained in the ultrasonic mixer.

In this study, it is required to consider, by technically improving the efficiency of heat transfer systems, that the influencing properties are specific heat capacity (SHC), thermal conductivity, pH range, viscosity, and dynamic viscosity. These properties were measured with calorimeter with differential scanning, thermal meter (KD2-Pro), pH meter, and viscometer (Brookfield), respectively. Before that the volume concentrations are significant aspects to measure the quantity of particles blended with base fluid or working fluid to maintain the thermophysical properties. The forecasted thermal conductivity of prepared nanofluids was not uniform [24].

Various techniques like transient hot wire (TWH) method, temperature oscillation, steady-state parallel plate, and optical beam and deflection were used to verify the thermal conductivity of nanofluids. Among these techniques, THW is a suited method to find out the thermal conductivity of composed SiO_2 nanofluids. The clustering and maximum temperature were highly impacted with modifications of thermal conductivity [25]. Similarly, the pH value was fine-tuned to improve the nanoparticles' dispersion evenly with the working fluid during the process. Finally, the thermal conductivity was carried with thermal meter (KD2-Pro) with Fourier's law in support of transfer-heat conduction [26]. Normally, the working base fluid thermal conductivity was much finer with lesser viscosity, and this viscosity is related with pumping force to affect the pressure fall. This test was conducted by the Brookfield viscometer (plate and cone type). The pH range and SHC were measured with pH meter and the differential scanning calorimeter. Meanwhile, simultaneously thermal conductivity has enhanced with moderate pH values [27]. The weight fraction of SiO_2, particle sizes, pH range, and sonication process time are the input factors which are displayed in Table 1.

3. Results and Discussion

3.1. Desirability Function Analysis on Processed Nanofluid Parameters. Based on the detailed processing procedures, thermophysical properties are obtained with appropriate processing parameters. There is need to validate the processing parameters to enhance the physical properties. Therefore, desirability approaches were used to identify the optimal process parameters. The composed nanofluids contain conditions like maximum thermal conductivity, minimum SHC, and viscosity [28]. The influenced process parameters are weight fraction of SiO_2, particle sizes, pH range, and sonication process time, and outcomes are thermal conductivity, SHC, and viscosity. The Taguchi L9 design was utilized to frame the processing levels [29]. The input aspects and its outcomes are displayed in Table 2 as per the L9 Taguchi technique.

3.2. Contour-Analysis of Thermal Properties with Input Factors

3.2.1. Contourplots of Weight Fraction and SiO_2 Particle Size on Thermal Properties. The contourplots of weight fraction of SiO_2 and particle size on the thermal conductivity, SHC and viscosity are displayed in Figures 3(a) and 3(b), respectively. From the figures, the thermal conductivity was increased at increasing of weight fraction 3%–4% and sizes of the particles were increased from 20 to 30 nm. Similarly, SHC, was enhanced with increase of weight fraction 3%–4% and low-level particle size 10 nm, and viscosity was improved at low-weight fraction and increase of particle sizes from 10 to 30 nm, respectively.

Table 1: Input factor for preparing nanofluids.

Process runs	Weight fraction of SiO_2 (vol.%)	SiO_2 reinforcement size (μm)	Water pH range	Sonication processing time
1	1.5	10	5	2
2	3	20	7	3
3	4.5	30	9	4

Table 2: Outcomes of thermal properties with L9 input.

Runs	Weight fraction of SiO_2	SiO_2 size	pH range (H_2O)	Sonication processing time (hr)	TC (W/mK)	SHC (J/kg K)	V (Cp)
1	2	10	5	0.2	0.9101	686	0.00145
2	3	10	7	0.4	0.9213	679	0.00168
3	4	10	9	0.6	0.9528	681	0.00194
4	2	20	9	0.4	0.9122	690	0.00159
5	3	20	5	0.6	0.9357	695	0.00174
6	4	20	7	0.2	0.9212	689	0.00152
7	2	30	7	0.6	0.9185	696	0.00146
8	3	30	9	0.2	0.9119	691	0.00151
9	4	30	5	0.4	0.9623	688	0.00162

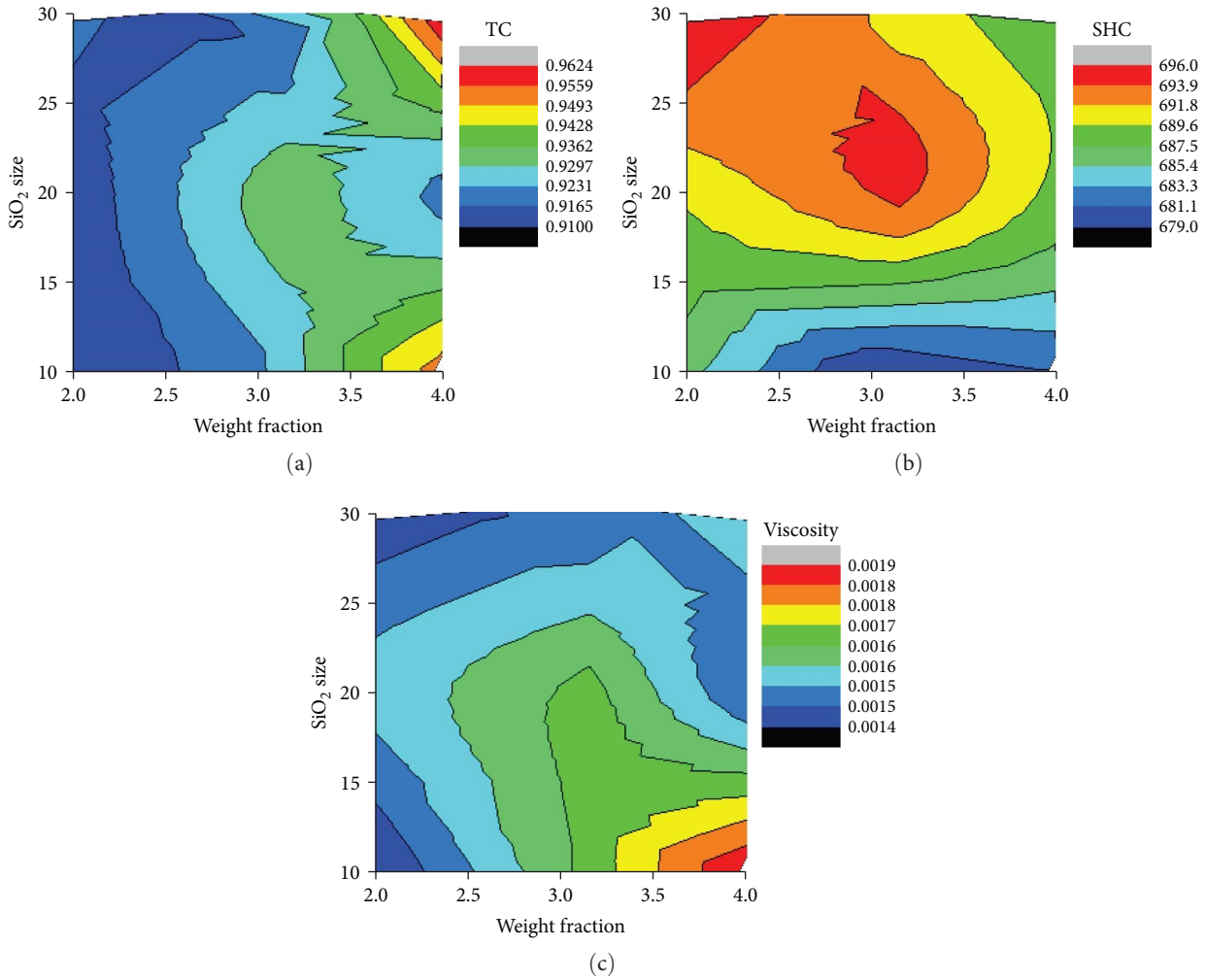

Figure 3: (a) Weight fraction and SiO_2 particle size on TC; (b) weight fraction and SiO_2 particle size on SHC; (c) weight fraction and SiO_2 particle size on viscosity.

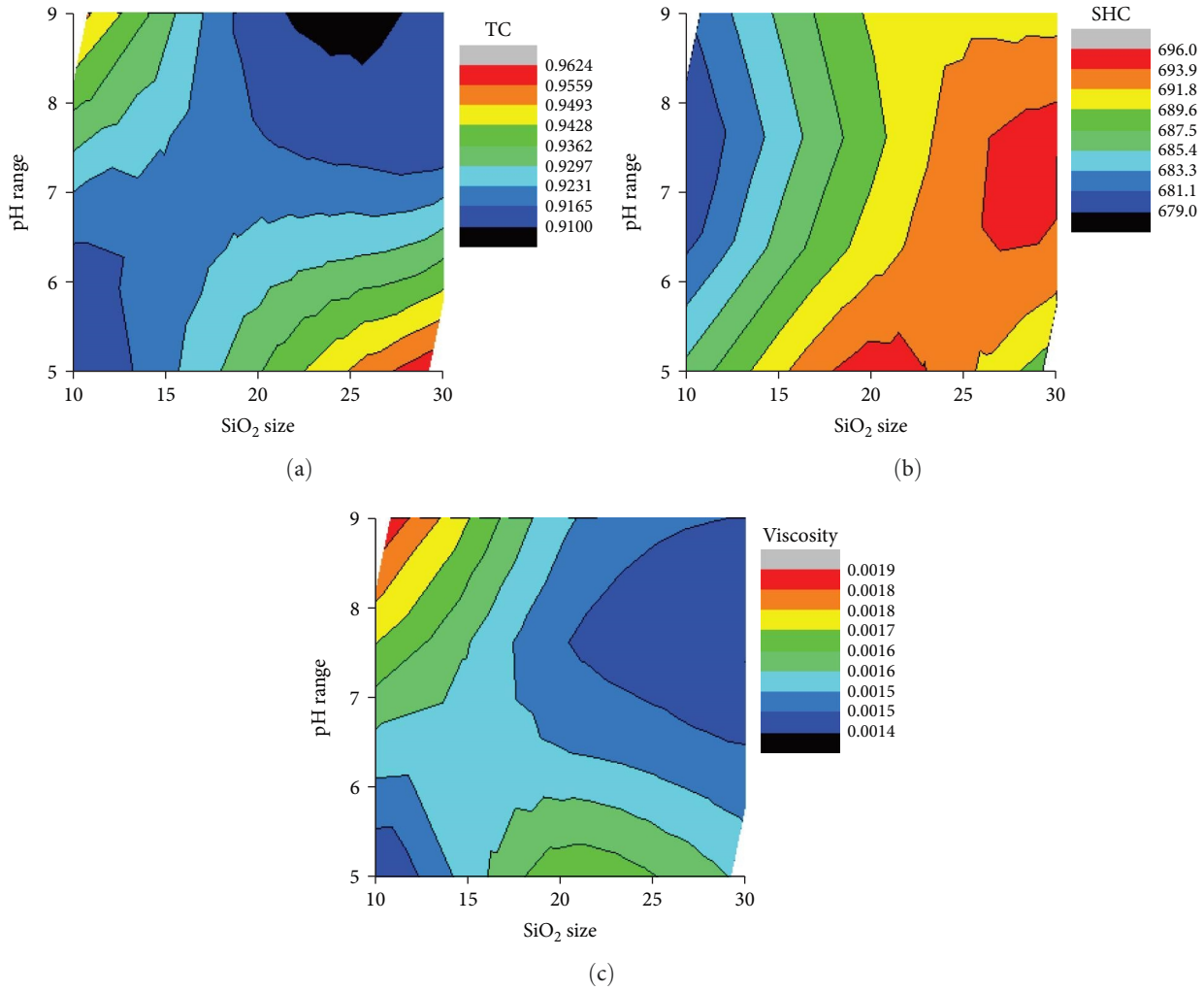

FIGURE 4: (a) SiO_2 particle sizes and pH range of water on TC; (b) SiO_2 particle sizes and pH range of water on SHC; (c) SiO_2 particle sizes and pH range of water on viscosity.

3.2.2. Contourplots of Particle Size of SiO_2 and pH Range on Thermal Properties. The contourplots of SiO_2 particle size and pH range on the thermal conductivity, SHC, and viscosity are displayed in Figures 4(a) and 4(b), respectively. From the figures, increase of particle size of SiO_2 and pH range from 7 to 9 improved the thermal conductivity. Meanwhile, decreasing the particle size of SiO_2 at 10 nm and raising the pH range from 7 to 9 enhanced the SHC. The viscosity was improved when the particle size was increased from 10–30 nm and pH range from 7 to 9.

3.2.3. Contourplots of pH Range of Water and Sonication Processing Time on Thermal Properties. Figure 5(a)–5(c) displays the contourplots pH range of water and processing of sonication on the thermal conductivity, SHC, and viscosity, respectively. From the figures, increase of pH range from 5 to 9 and processing time from low level (0.2) to medium level (0.4) enhanced the thermal conductivity. The SHC was improved on increasing the pH range from 7 to 9 and with low-level processing time. The viscosity was superior on increasing the pH range from 5 to 9 and processing time from 0.4 to 0.6 hr.

3.2.4. Contourplots of Sonication Processing Time and Weight Fraction of SiO_2 on Thermal Properties. Figure 6(a)–6(c) exhibited the contour plots sonication processing with durations and weight fraction on the thermal conductivity, SHC and viscosity, respectively. From the figures, it is understood that the thermal conductivity was improved at high level of processing time (0.6 hr) and weight fraction was increased from low (2.0) to moderate level (3.0). The SHC was enhanced at low level of processing time (0.2) to moderate level (0.4) and weight fraction from (2.0% to 3.0%). Finally, viscosity level was enhanced at low level processing time and low level weight fraction.

3.2.5. Contourplots of Desirability on the Thermal Properties of Nanofluid SiO_2. In this study, desirability was approached on the thermal properties to find out the optimal process parameters. Before that the input factors were arranged in the Taguchi design with L9 array as per the discussion in Materials and Method section. The main objective of this desirability is to convert the multiresponses into a single response for better understanding. During the desirability, the outcomes like thermal conductivity at

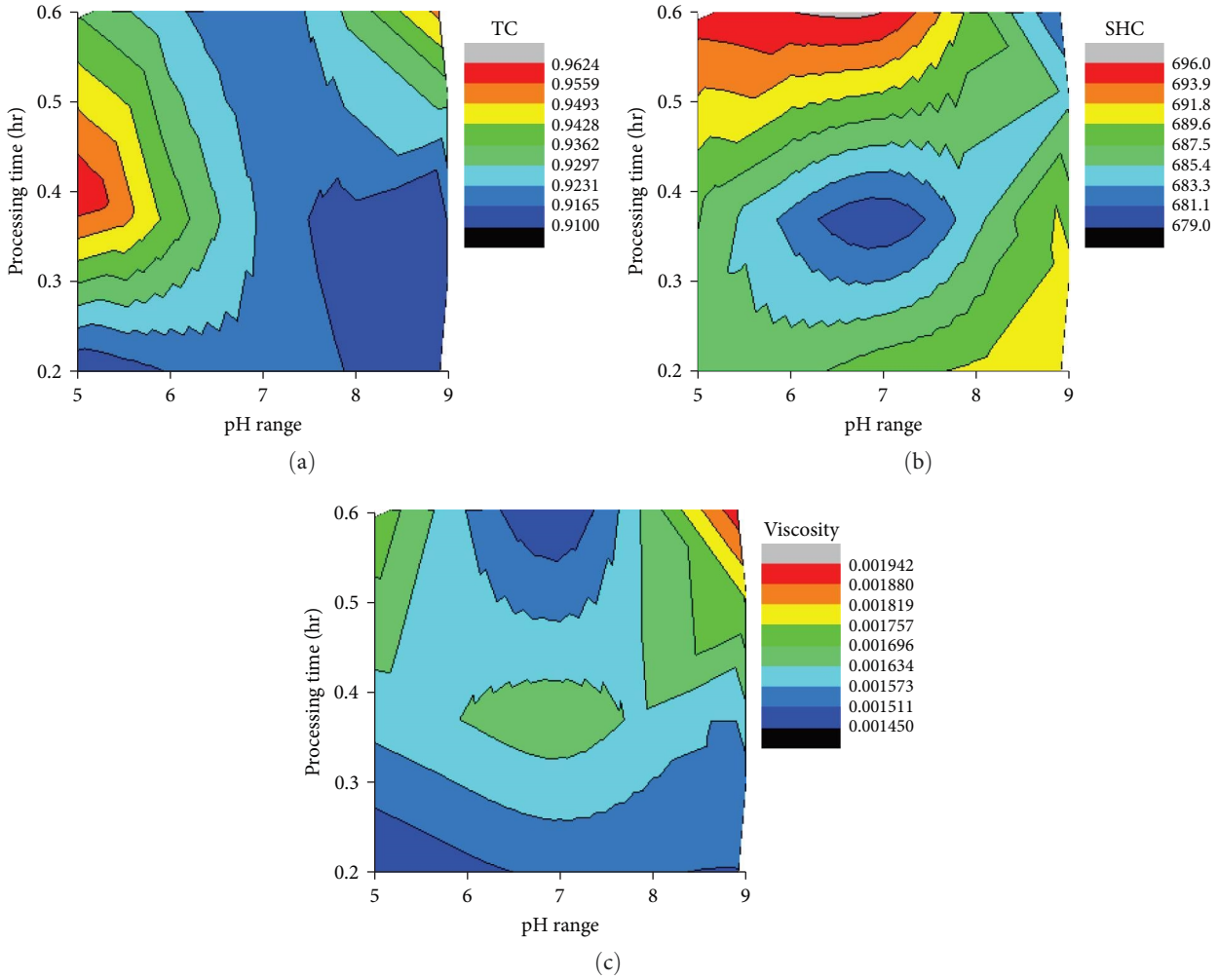

FIGURE 5: (a) pH range of water and processing time on TC; (b) pH range of water and processing time on SHC; (c) pH range of water and processing time on viscosity.

maintaining the maximum the better concept, and SHC and viscosity were considered as the smaller the better condition, respectively. Normalized signal to noise ratios of thermal conductivity, SHC, and viscosity values and other related values of desirability coefficient and its composite desirability values are listed in Table 3. From Table 3, the ranking methods from the weight of 0.5 values were used to find out the ranking procedures. Experimental runs show that the 9th sample gives a better rank. Optimum process parameters found that weight fraction 4%, 30 nm of particles of SiO_2, pH-5 range and 0.4 hr of sonication processing. The ranking graph and its overall processing runs are displayed in Figure 7. The metal oxide of SiO_2 achieved better thermal conductivity, SHC, and viscosity as mentioned ranges.

4. Convective Heat Transfer with Prepared Nanofluids through Straight Tube

Based on the L9 array, desirability functions were used to compose better optimal process parameters. Now these parameters were analyzed to carry out the convective heat transfer with straight tube heat transfer section with specialized parameters. The designed heat-transfer system was a loop section which contained nanofluid reservoir, nanofluid pump, flow meter, the chambers having heater, insulator, K-thermocouple, and manometer, and another section contained cooling water reservoir, flow meter, cooling water pump, and heat exchanger.

The copper-made tube was used with heat-transfer test chamber with thickness of 2.5 mm, inner diameter of 8.2 mm, and length of 0.873 m, respectively. The thermocouples having K-type design with 0.2°C precisions were maintained with wall temperature. Similarly, the two types of T-thermocouples were maintained at same precision as mentioned in K-type to estimate the bulk temperature on both sides of the sections. Throughout the process, constant heat flux condition was attained with electrically heated transfer condition using power supply. The heat exchanger with plate design was used to locate the inlet temperature in the range of 26+ or −1°C and the volume-flow rate was calculated by the flow meter with 0.02 L/min precision.

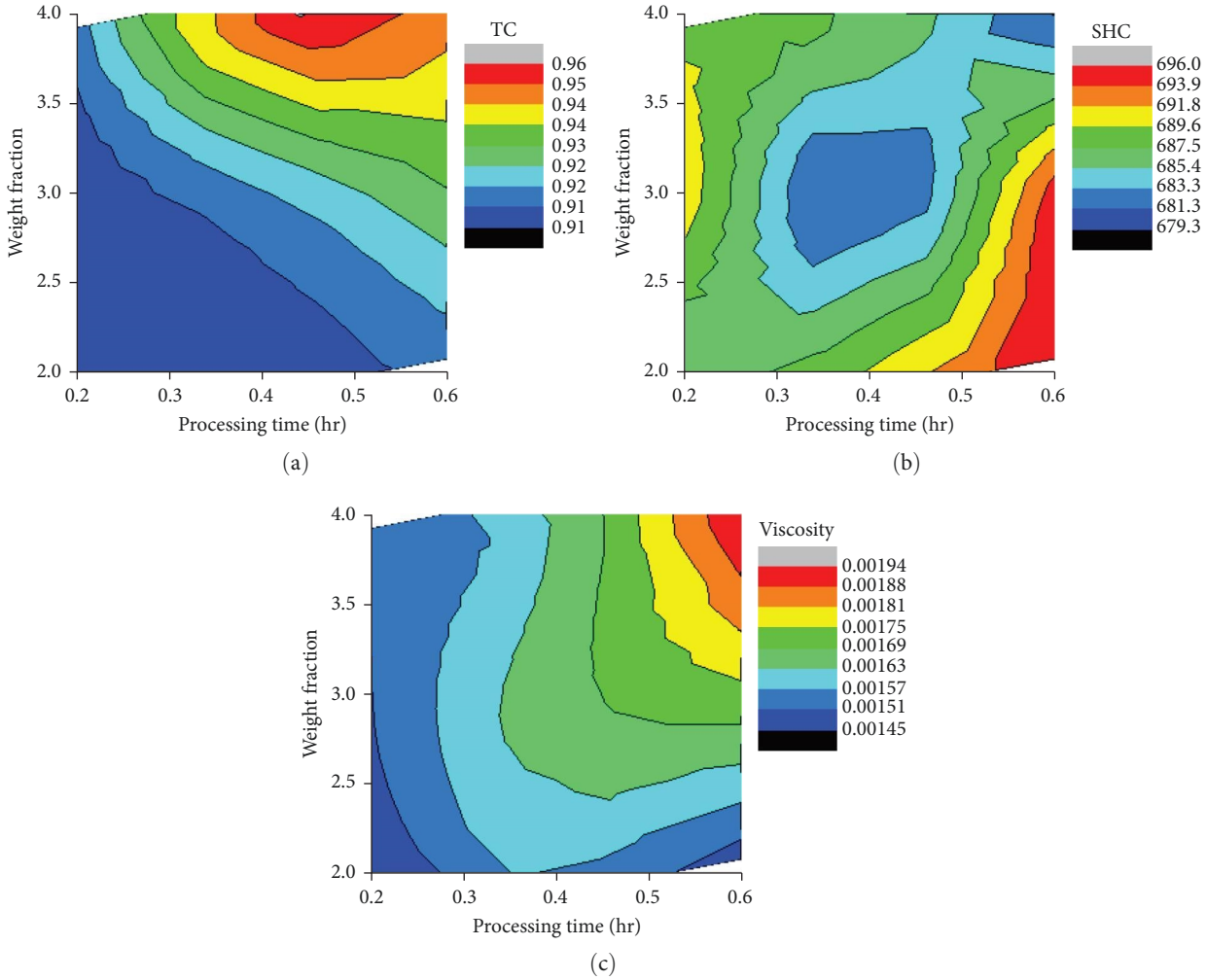

Figure 6: (a) Processing time and weight fraction of SiO_2 on TC; (b) processing time and weight fraction of SiO_2 on SHC; (c) processing time and weight fraction of SiO_2 on viscosity.

Table 3: Desirability values with their input factors and thermal outcomes.

Run	Signal to noise ratios—Normalized			DFA-coefficient			DFA	Grade
	TC	SHC	V	TC	SHC	V		
1	1.0000	−0.5882	−1.0000	0.0000	1.5882	2.0000	0.0000	9
2	0.7854	−1.0000	−0.5306	0.2146	2.0000	1.5306	0.8104	4
3	0.1820	−0.8824	0.0000	0.8180	1.8824	1.0000	1.2409	2
4	0.9598	−0.3529	−0.7143	0.0402	1.3529	1.7143	0.3055	7
5	0.5096	−0.0588	−0.4082	0.4904	1.0588	1.4082	0.8551	3
6	0.7874	−0.4118	−0.8571	0.2126	1.4118	1.8571	0.7467	5
7	0.8391	0.0000	−0.9796	0.1609	1.0000	1.9796	0.5644	6
8	0.9655	−0.2941	−0.8776	0.0345	1.2941	1.8776	0.2895	8
9	0.0000	−0.4706	−0.6531	1.0000	1.4706	1.6531	1.5592	1

4.1. Data Processing. As per the required formula, density and specific heat properties were found with help of mixture characteristics of nanofluids, and assuming the thermal equilibrium among the nanoparticle SiO_2 and working fluid, the SHC and thermal conductivity were also identified and optimal parameters were pointed out. Next to the total heat flux finding, $Q1$ and $Q2$ were found with heat input values.

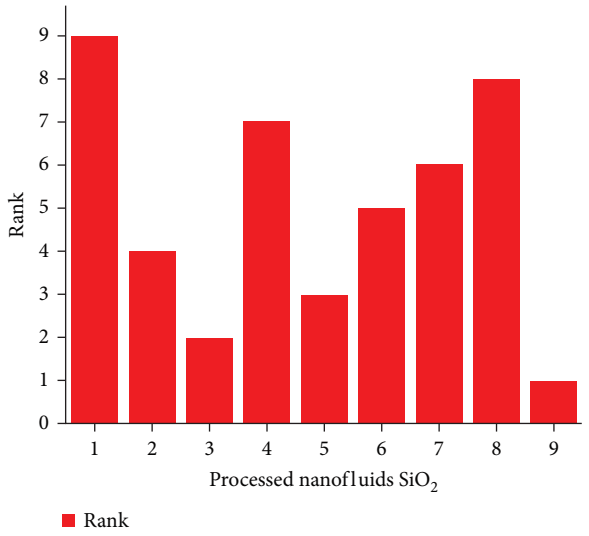

Figure 7: Nanofluids SiO_2 and DFA rank.

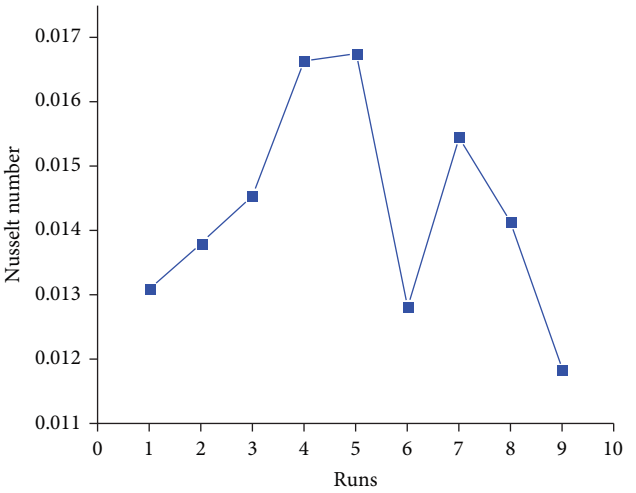

Figure 8: Various runs of nanofluids and Nusselt number.

Table 4: Heat transfer coefficient, Nusselt and Reynolds number.

Runs	TC (W/mK)	SHC (J/kg K)	V (Cp)	Fluid velocity (m/s)	Heat transfer coefficient (W/m^2 K)	Nusselt number	Reynolds number
1	0.9101	686	0.00145	0.36	1.45	0.013092	2.035862
2	0.9213	679	0.00168	0.52	1.55	0.013796	2.538095
3	0.9528	681	0.00194	0.81	1.69	0.014545	3.423711
4	0.9122	690	0.00159	0.59	1.85	0.01663	3.042767
5	0.9357	695	0.00174	0.458	1.91	0.016738	2.158391
6	0.9212	689	0.00152	0.235	1.44	0.012818	1.267763
7	0.9185	696	0.00146	0.67	1.73	0.015445	3.763014
8	0.9119	691	0.00151	0.298	1.57	0.014118	1.618278
9	0.9623	688	0.00162	0.369	1.39	0.011845	1.867778

$$\text{Total heat flux } (q) = \frac{\text{Heat Input from heater (Q1)} + \text{Heat Input to the fluid (Q2)}}{2\pi DL}, \tag{1}$$

$$\text{Heat transfer coefficient } (h) = \frac{\text{Total heat flux } (q)}{\text{axial length (wall temperature} - \text{bulk temperature)}}. \tag{2}$$

Similarly, heat transfer coefficient was found in the Equation (1) and by the heat temperatures with wall and fluids bulk temperature and axial length (x) from the inlet of the heat transfer. The Nusselt number was identified from the heat flux, tube diameter from thermal conductivity, and the Reynolds number was employed with velocity, diameter of the pipe, and kinematic viscosity. Equations (3) and (4) exhibit the Nusselt and Reynolds number formulas.

$$\text{Nusselt number} = \frac{hD}{\text{Thermal conductivity } (K)}, \tag{3}$$

$$\text{Reynolds number} = \frac{\text{Density of the fluid} \times \text{fluid velocity} \times \text{diameter of pipe}}{\text{Viscosity } (V)}. \tag{4}$$

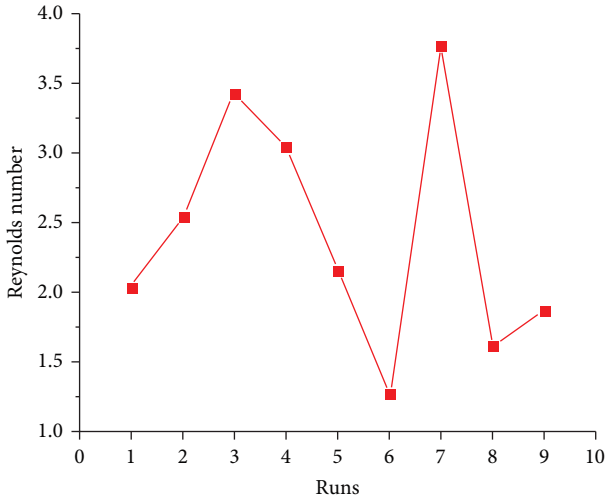

Figure 9: Various runs of nanofluids and Reynolds number.

From the entire equations, the heat transfer coefficients, and Nusselt and Reynolds numbers were identified with output responses like thermal conductivity and viscosity. These number outcomes and heat-transfer coefficient values were employed with L9 table. Table 4 exhibits the heat-transfer coefficients, and Nusselt and Reynolds numbers with convective heat transfer throughout the straight tube with specified conditions.

Figures 8 and 9 show the various runs of nano-SiC fluids and Nusselt and Reynolds numbers. From the figures, it is clear that the correlations of different process parameters and numbers were clearly noted. From the Reynolds number, the attained values are <2,000 ranges so that the flows are related with laminar flow. From the figures, it is implicit that the fifth and seventh runs attained highest values.

5. Conclusion

(1) In this investigation, preparation of SiO_2 nanofluids were successfully carried with two-step technique.

(2) The desirability function was approached effectively to improve the efficiency of thermal properties with appropriate process parameters.

(3) The weight fraction of SiO_2, particle sizes, pH range of water, and sonication processing durations were most influenced input parameters to thermal properties.

(4) The contour analysis between the input parameters of two-step method and their outcomes like thermal conductivity, SFC, and viscosity was detailed in analysis.

(5) The superior thermal physical properties are 0.9623 W/mK for thermal conductivity, 688 J/kg K for SHC, and 0.00162 for viscosity, respectively.

(6) The heat-transfer coefficient was successfully identified with total heat flux and axial dimensions. The designed heat-transfer system was effectively employed with selected design parameters and heat-transfer coefficient.

(7) The heat-transfer section will be expanded and more thermocouples will be added in the planned design and implement in the further studies.

Data Availability

The data used to support the findings of this study are included within the article. Further data or information are available from the corresponding author upon request.

Conflicts of Interest

The authors declare that they have no conflicts of interest.

References

[1] G. Jena, R. P. George, and J. Philip, "Fabrication of a robust graphene oxide-nano SiO_2-polydimethylsiloxane composite coating on carbon steel for marine applications," *Progress in Organic Coatings*, vol. 161, Article ID 106462, 2021.

[2] W.-H. Chen, Y.-F. Wang, Z.-P. He, and M.-C. Ding, "Stability, rheology and displacement performance of nano-SiO_2/HPAM/NaCl dispersion systems," *Journal of Fuel Chemistry and Technology*, vol. 48, no. 5, pp. 568–576, 2020.

[3] D. Veeman, M. Swapna Sai, P. Sureshkumar et al., "Additive manufacturing of biopolymers for tissue engineering and regenerative medicine: an overview, potential applications, advancements, and trends," *International Journal of Polymer Science*, vol. 2021, Article ID 4907027, 20 pages, 2021.

[4] K. N. Koutras, A. E. Antonelou, I. A. Naxakis, V. P. Charalampakos, E. C. Pyrgioti, and S. N. Yannopoulos, "*In-situ* high temperature study of the long-term stability and dielectric properties of nanofluids based on TiO_2 and SiC dispersions in natural ester oil at various concentrations," *Journal of Molecular Liquids*, vol. 359, Article ID 119284, 2022.

[5] R. Tadepalli, R. K. Gadekula, K. V. Reddy et al., "Characterization of thermophysical properties of Al_2O_3, TiO_2, SiO_2, SiC and CuO nano particles at cryogenic temperatures," *Materials Today: Proceedings*, vol. 5, Part 2, no. 14, pp. 28454–28461, 2018.

[6] S. Yogeshwaran, R. Prabhu, L. Natrayan, and R. Murugan, "Mechanical properties of leaf ashes reinforced aluminum alloy metal matrix composites," *International Journal of Applied Engineering Research*, vol. 10, no. 13, pp. 11048–11052, 2015.

[7] Z. A. Nawsud, A. Altouni, H. S. Akhijahani, and H. Kargarsharifabad, "A comprehensive review on the use of nano-fluids and nano-PCM in parabolic trough solar collectors (PTC)," *Sustainable Energy Technologies and Assessments*, vol. 51, Article ID 101889, 2022.

[8] M. H. Esfe and A. A. A. Arani, "An experimental determination and accurate prediction of dynamic viscosity of MWCNT (%40)-SiO_2(%60)/5W50 nano-lubricant," *Journal of Molecular Liquids*, vol. 259, pp. 227–237, 2018.

[9] L. Natrayan and M. S. Kumar, "Influence of silicon carbide on tribological behaviour of AA2024/Al_2O_3/SiC/Gr hybrid metal matrix squeeze cast composite using Taguchi technique," *Materials Research Express*, vol. 6, no. 12, Article ID 1265f9, 2020.

[10] A. A. Abed, O. K. Ahmed, M. M. Weis, and K. I. Hamada, "Performance augmentation of a PV/Trombe wall using Al_2O_3/water nano-fluid: an experimental investigation," *Renewable Energy*, vol. 157, pp. 515–529, 2020.

[11] N. Kana, A. Galmed, T. Khamliche, K. Kaviyarasu, and M. Maaza, "Thermal conductivity enhancement in MoO_3–H_2O nano-sheets based nano-fluids," *Materials Today: Proceedings*, vol. 36, Part 2, pp. 379–382, 2021.

[12] M. Senthil Kumar, L. Natrayan, R. D. Hemanth, K. Annamalai, and E. Karthick, "Experimental investigations on mechanical and microstructural properties of Al_2O_3/SiC reinforced hybrid metal matrix composite," *IOP Conference Series: Materials Science and Engineering*, vol. 402, Article ID 012123, 2018.

[13] S. Mukherjee and S. Paria, "Preparation and stability of nanofluids-a review," *IOSR Journal of Mechanical and Civil Engineering*, vol. 9, no. 2, pp. 63–69, 2013.

[14] M. Sandhya, D. Ramasamy, K. Sudhakar, K. Kadirgama, and W. S. W. Harun, "Ultrasonication an intensifying tool for preparation of stable nanofluids and study the time influence on distinct properties of graphene nanofluids–a systematic overview," *Ultrasonics Sonochemistry*, vol. 73, Article ID 105479, 2021.

[15] A. Merneedi, L. Natrayan, S. Kaliappan et al., "Experimental investigation on mechanical properties of carbon nanotube-reinforced epoxy composites for automobile application," *Journal of Nanomaterials*, vol. 2021, Article ID 4937059, 7 pages, 2021.

[16] N. H. Abu-Hamdeh, R. A. Alsulami, A. A. Aljinaidi et al., "Numerical investigation of molten salt/SiO_2 nano-fluid in the solar power plant cycle and examining different arrangements of shell and tube heat exchangers and plate heat exchangers in these cycles," *Journal of the Taiwan Institute of Chemical Engineers*, vol. 124, pp. 1–8, 2021.

[17] S. K. Singh, S. K. Verma, and R. Kumar, "Thermal performance and behavior analysis of SiO_2, Al_2O_3 and MgO based nano-enhanced phase-changing materials, latent heat thermal energy storage system," *Journal of Energy Storage*, vol. 48, Article ID 103977, 2022.

[18] Y. S. Jang, T. Oh, N. Banthia, and D.-Y. Yoo, "Effects of nano-SiO_2 coating and induced corrosion of steel fiber on the interfacial bond and tensile properties of ultra-high-performance concrete (UHPC)," *Journal of Building Engineering*, vol. 54, Article ID 104637, 2022.

[19] Q. Yu, Y. Lu, C. Zhang, X. Zhang, Y. Wu, and A. Sciacovelli, "Preparation and thermal properties of novel eutectic salt/nano-SiO_2/expanded graphite composite for thermal energy storage," *Solar Energy Materials and Solar Cells*, vol. 215, Article ID 110590, 2020.

[20] Z. Iqbal, E. Azhar, and E. N. Maraj, "Performance of nanopowders SiO_2 and SiC in the flow of engine oil over a rotating disk influenced by thermal jump conditions," *Physica A: Statistical Mechanics and its Applications*, vol. 565, Article ID 125570, 2021.

[21] M. H. Esfe, S. Saedodin, and D. Toghraie, "Experimental study and modeling the SiO_2-MWCNT (30:70)/SAE40 hybrid nanolubricant flow based on the response surface method to identify the optimal lubrication conditions," *International Communications in Heat and Mass Transfer*, vol. 130, Article ID 105771, 2022.

[22] M. Awais, A. A. Bhuiyan, S. Salehin, M. M. Ehsan, B. Khan, and Md. H. Rahman, "Synthesis, heat transport mechanisms and thermophysical properties of nanofluids: a critical overview," *International Journal of Thermofluids*, vol. 10, Article ID 100086, 2021.

[23] M. H. Esfe, S. Saedodin, O. Mahian, and S. Wongwises, "Thermal conductivity of Al_2O_3/water nanofluids," *Journal of Thermal Analysis and Calorimetry*, vol. 117, pp. 675–681, 2014.

[24] X.-J. Wang and X.-F. Li, "Influence of pH on nanofluids' viscosity and thermal conductivity," *Chinese Physics Letters*, vol. 26, no. 5, Article ID 056601, 2009.

[25] S. Tian, W. Gao, Y. Liu, W. Kang, and H. Yang, "Effects of surface modification nano-SiO_2 and its combination with surfactant on interfacial tension and emulsion stability," *Colloids and Surfaces A: Physicochemical and Engineering Aspects*, vol. 595, Article ID 124682, 2020.

[26] S. A. Asiri, E. M. Salilih, K. M. Alfawaz, A. F. Alogla, S. M. Sajadi, and O. K. Nusier, "Transient heat transfer analysis of serially connected array of phase change material in the thermal battery units with Al_2O_3 working nano fluids," *Journal of Energy Storage*, vol. 53, Article ID 105184, 2022.

[27] C. Rajaganapathy, T. V. Rajamurugan, A. D. Bruno, S. Murugapoopathi, and M. Armstrong, "A study on tribological behavior of rice bran and karanja oil-based TiO_2 nano bio-fluids," *Materials Today: Proceedings*, vol. 57, Part 1, pp. 125–129, 2022.

[28] K. S. Suganthi and K. S. Rajan, "Metal oxide nanofluids: review of formulation, thermo-physical properties, mechanisms, and heat transfer performance," *Renewable and Sustainable Energy Reviews*, vol. 76, pp. 226–255, 2017.

[29] G. Deshmukh, N. Jose, R. Shidhav, A. Suryawanshi, R. Datir, and M. R. Ravindra, "Nanofluids: an introduction to new generation heat transfer fluids," *Acta Scientific Agriculture*, vol. 3, no. 2, pp. 41–48, 2019.